Journal of Crystal Growth 418 (2015) 1–6

Contents lists available at ScienceDirect

Journal of Crystal Growth

journal homepage: www.elsevier.com/locate/jcrysgro

Growth of single-crystals of rare-earth zirconate pyrochlores, $Ln_2Zr_2O_7$ (with Ln=La, Nd, Sm, and Gd) by the floating zone technique

M. Ciomaga Hatnean*, M.R. Lees, G. Balakrishnan*

Department of Physics, University of Warwick, Coventry CV4 7AL, UK

ARTICLE INFO

Article history:
Received 7 October 2014
Received in revised form
28 January 2015
Accepted 31 January 2015
Communicated by K. Jacobs
Available online 7 February 2015

Keywords:
A2. Floating zone technique
A2. Single crystal growth
B1. Rare-earth zirconate
B1. Pyrochlore
B1. Fluorite
B2. Frustrated magnets

ABSTRACT

The geometrical frustration occurring in the crystal lattice of pyrochlore oxides of the type $A_2B_2O_7$ (where A=Rare Earth, B=Mo, Sn, Ti, Zr) leads to exotic magnetic properties of these materials. The present study focuses on a new class of frustrated magnets, the lanthanide zirconates. Large, high quality single-crystals of the rare-earth zirconium oxides, $Ln_2Zr_2O_7$ (where Ln=La, Nd, Sm, and Gd), have been grown by the floating zone technique, using a high power xenon arc lamp furnace. The crystals have been characterized and tested for their quality using X-ray diffraction techniques.

1. Introduction

Pyrochlore oxides, $A_2^{3+}B_2^{4+}O_7$ (where A= trivalent rare-earth metal, B= tetravalent transition metal), have been thoroughly investigated over the past two decades, both theoretically and experimentally [1]. The stability field diagram established by Subramanian et al. shows a wide array of elements (both for the A and B sites) form as the $A_2^{3+}B_2^{4+}O_7$ pyrochlore phase [2]. The geometrically frustrated network of corner sharing tetrahedra of the metal ion sites (both A and B sites) and the nature of these ions leads to a large variety of unusual magnetic behaviors [1].

Considerable progress has been made in the field of frustrated magnetism due to breakthroughs in the preparation of large, high quality single-crystals of various pyrochlores. It was first shown that large single crystals of the rare-earth titanate pyrochlores $A_2^{3+}Ti_2O_7$ (where A= Pr, Nd, Sm, Tb, Dy, Ho, Er, Y) could be produced by the floating zone technique [3,4]. Subsequently, crystals of the entire series of rare-earth titanates $A_2^{3+}Ti_2O_7$ (A=Pr→Lu) [5–8] were grown, their structural and magnetic properties investigated in detail, and their magnetic ground states elucidated [6,7,9–11]. Recently, crystals of the molybdate family, $A_2Mo_2O_7$ (where A=Nd, Sm, Gd, Tb, Dy) [12,13], have also been grown using the floating zone technique and their properties studied [13–17].

The research community has recently shown an increased interest in the lanthanide zirconates, $Ln_2Zr_2O_7$, both due to their potential use in the immobilization of radioactive waste [18] and in thermal barrier coatings [19], and in the quest for materials which exhibit quantum spin liquid or quantum spin ice behavior [20,21]. Lanthanide zirconium oxides crystallize in the cubic structure at room temperature and at ambient pressures. Nevertheless, depending on the ionic radius ratio of the two metallic ions, RR = $(r_{Ln^{3+}}/r_{Zr^{4+}})$, their structure can be stabilized with one of two different space groups, either $Fd\bar{3}m$ (No. 227), which corresponds to the pyrochlore structure (large lanthanide elements), or $Fm\bar{3}m$ (No. 225), belonging to the defect-fluorite structure (for small lanthanide elements) [2].

Lanthanide zirconates, $Ln_2Zr_2O_7$ (with Ln = Tb→Lu), with the ionic radius ratio, RR, ranging from 1.44 to 1.35, crystallize in a defect-fluorite structure [2]. Compounds $Ln_2Zr_2O_7$ (where Ln = La→Gd), with the ionic radius ratio, RR, ranging from 1.61 to 1.46, adopt the cubic pyrochlore structure [2]. Their crystallographic structure contains two different cation sites and two distinct anion sites; the large trivalent rare-earth Ln^{3+} ions occupy the eight-fold oxygen coordinated A sites, while the six-fold coordination of the B sites is filled by the smaller tetravalent zirconium ions Zr^{4+} [2].

At high temperature (T > 1500 °C), lanthanide zirconates $Ln_2Zr_2O_7$ (where Ln = Nd→Gd) undergo an order–disorder transition from a pyrochlore to a defect-fluorite structure. The transition temperature depends on the nature of the rare-earth ion [2,22–24]. Therefore,

* Corresponding authors.
E-mail addresses: M.Ciomaga-Hatnean@warwick.ac.uk (M. Ciomaga Hatnean), G.Balakrishnan@warwick.ac.uk (G. Balakrishnan).
URL: http://go.warwick.ac.uk/supermag (G. Balakrishnan).

http://dx.doi.org/10.1016/j.jcrysgro.2015.01.037
0022-0248/

lanthanum zirconate exists only in the pyrochlore form, whereas for neodymium, samarium, and the gadolinium zirconates, a transition from a pyrochlore to a defect-fluorite structure occurs at 2300, 2000, and 1530 °C respectively [22]. Furthermore, recent studies have shown that the lanthanide zirconates with a pyrochlore structure are not stable at high pressure and that they undergo a pressure induced structural transformation leading to either a monoclinic phase (space group $P2_1/c$) [25,26], or a defect cotunnite-type structure (space group *Pnma*) [27].

Due to the high melting point of the lanthanide zirconate pyrochlores [28], it has proven difficult to obtain crystals of these materials and until recently the structural and magnetic properties of this new class of pyrochlore oxides have only been studied using powder samples [22,23,29–35].

Roth showed in a previous study of the phase diagram of Ln_2O_3–ZrO_2 (where Ln=La and Nd) [28] that the pyrochlore type oxides melt congruently above 2000 °C. Single-crystals of the zirconates pyrochlore family can therefore be grown by the floating zone technique but due to the high melting point of these oxides, the crystal growth using optical furnaces can only be carried out with a high power xenon arc lamp furnace.

In this paper, we report the growth, for the first time, of single-crystals of the lanthanide zirconates pyrochlores, $Ln_2Zr_2O_7$ (where Ln=La, Nd, Sm, and Gd). Recent studies [20,36–38] have shown the feasibility of the floating zone technique for preparing single-crystals of one member of the zirconate family, $Pr_2Zr_2O_7$. The present study demonstrates that large, high quality crystals of a number of pyrochlore lanthanide zirconates may be grown using this technique. This is especially important for the study of the properties of this new class of geometrically frustrated magnets and particularly for solving the nature of their magnetic ground states.

2. Experimental details

The $Ln_2Zr_2O_7$ (where Ln=La, Nd, Sm, and Gd) pyrochlore oxides were first synthesized in polycrystalline form by reacting powders of the starting oxides, Ln_2O_3 (99.9%) and ZrO_2 (99%). Stoichiometric amounts of the powders were ground together and calcined in air for several days at temperatures in the range 1300–1450 °C with intermediate grindings. The resulting material was then isostatically pressed into rods (typically 6–8 mm diameter and 70–80 mm long) and sintered at 1450–1600 °C in air for several days. X-ray diffraction patterns of powdered pieces of the rods were recorded on a Panalytical X-Ray diffractometer with a Cu Kα_1 anode (λ=1.5406 Å). The diffraction patterns were collected at room temperature and over an angular range of 10–110° 2θ with a step size of 0.013° in 2θ and a total scanning time of 16 h. The analysis of the X-ray patterns was performed using the Fullprof software suite [39].

Crystals of the lanthanide zirconate, $Ln_2Zr_2O_7$, were grown in air or in oxygen atmospheres. The growths were carried out in a four-mirror xenon arc lamp optical image furnace (CSI FZ-T-12000-X_VI-VP, Crystal Systems Incorporated, Japan), at growth speeds in the range 5–15 mm/h. Initially, polycrystalline rods were used as seeds and once good quality crystals were obtained, a crystal seed was used for subsequent growths. The two rods (feed and seed) were counter-rotated at a rate of 20–30 rpm.

To analyze the microstructure and to investigate the crystal perfection of the floating zone-grown crystals, pieces of the $Nd_2Zr_2O_7$ boules were cut along the growth direction, polished and studied using polarized light microscopy.

The quality of the as-grown crystals was checked using a Laue X-ray imaging system with a Photonic-Science Laue camera system.

Small quantities of each crystal were ground into powder and powder X-ray diffraction measurements were performed to determine the phase purity and to establish the crystallographic structure of the $Ln_2Zr_2O_7$ crystals. It is important to determine whether the lanthanide zirconates boules have crystallized in either the pyrochlore or the defect-fluorite phase. Room temperature diffractograms were collected on a Bruker D5005 X-ray diffractometer using Cu Kα_1 and Kα_2 radiation ($\lambda_{K\alpha1}$ = 1.5406 Å and $\lambda_{K\alpha2}$ = 1.5444 Å), between 10° and 110° 2θ, with a step size of 0.016° in 2θ, and a total scanning time of 24 h. The patterns were then analyzed using the Fullprof software suite [39].

3. Results and discussion

Lanthanide zirconate $Ln_2Zr_2O_7$ (where Ln=La, Nd, Sm, and Gd) crystals were grown by the floating zone method, using different growth conditions. A summary of the conditions used is given in Table 1. All the Zr-based pyrochlores grown appear to melt congruently and little or no evaporation was observed for any of the growths. Crystals of $Ln_2Zr_2O_7$ were successfully grown using various growth rates, however larger monocrystalline samples were isolated from the crystal boules prepared using higher growth speeds. In the following sections, we describe the crystal growth of each lanthanide zirconate.

3.1. $La_2Zr_2O_7$

$La_2Zr_2O_7$ feed rods were sintered at 1550 °C in air for 2 days. Analysis of room temperature powder X-ray diffraction patterns collected on powdered sections of the polycrystalline rods provided a good fit

Table 1
Summary of the conditions used for the growth of $Ln_2Zr_2O_7$ (where Ln= La, Nd, Sm, and Gd) crystals. All the boules grown were transparent to light.

$Ln_2Zr_2O_7$	Growth rate (mm/h)	Atmosphere	Pressure	Rod rotation rate (rpm)	Color of crystal boule
$La_2Zr_2O_7$	12.5–15	Air	Ambient	20–30	Colorless
$Nd_2Zr_2O_7$	10–15	Air	Ambient	20–30	Dark-purple
$Sm_2Zr_2O_7$	5–15	O_2	4 bars	20–30	Light-orange
$Gd_2Zr_2O_7$	10–15	Air	Ambient	20–30	Light-yellow

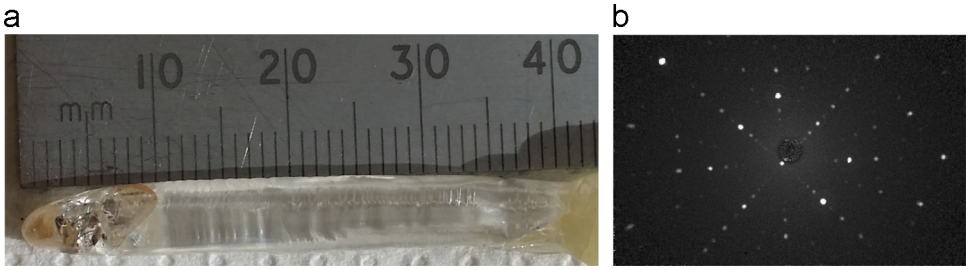

Fig. 1. (a) Boule of $La_2Zr_2O_7$ prepared by the floating zone method in air at a growth rate of 15 mm/h. (b) X-ray Laue back reflection photograph taken for one of the facets of a $La_2Zr_2O_7$ crystal.

to the pyrochlore structure (space group $Fd\bar{3}m$). In addition, no unindexed reflections were observed on the X-ray profile of the powdered rods.

The lanthanum zirconate crystals prepared by the floating zone technique were typically 5–7 mm in diameter and 30–50 mm long. The crystals developed facets as they grew and two very strong facets were present on almost the entire length of most of the grown crystals. Fig. 1a shows a photograph of a crystal of $La_2Zr_2O_7$, which was grown in air at a growth speed of 15 mm/h.

X-ray Laue photographs taken of boules of $La_2Zr_2O_7$ (see Fig. 1b) confirm the high quality of the crystals. The Laue patterns indicate that the [1 0 0] direction is nearly orthogonal to one of the facets on the sides of the as-grown crystal boules.

The X-ray diffraction profile of the powder from a single crystal of $La_2Zr_2O_7$, shown in Fig. 2, reveals the presence of some low-angle weak superlattice reflections (with ($h\,k\,l$)=(1 1 1), (3 3 1), and (5 1 1)), which are a distinct feature of the pyrochlore-type structure [35]. All the peaks observed could be indexed in the cubic $Fd\bar{3}m$ space group (see Table 2 for the goodness of fit value), and no impurity peaks were observed in the patterns.

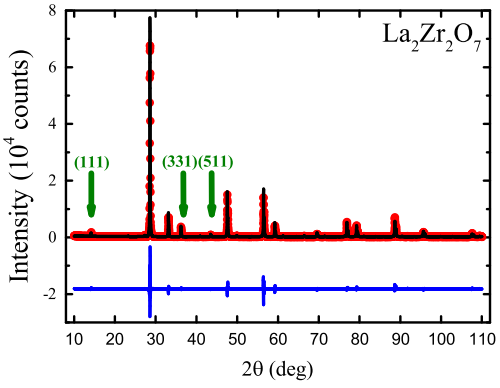

Fig. 2. Room temperature powder X-ray diffraction pattern collected on a ground boule of $La_2Zr_2O_7$. The experimental profile (red closed circles) and a full profile matching refinement (black solid line) made using the $Fd\bar{3}m$ cubic structure are shown, with the difference given by the blue solid line. The pyrochlore superlattice reflections (1 1 1), (3 3 1) and (5 1 1) are indicated by the green arrows. (For interpretation of the references to color in this figure caption, the reader is referred to the web version of this paper.)

Table 2
Lattice parameters for $Ln_2Zr_2O_7$ (where Ln= La, Nd, Sm, and Gd), refined from the room temperature powder X-ray diffraction data.

Z	Ln	Crystal structure type	Space group	a (Å)	GOF
57	La	Pyrochlore	$Fd\bar{3}m$	10.79921(6)	3.22
60	Nd	Pyrochlore	$Fd\bar{3}m$	10.61337(8)	2.28
62	Sm	Pyrochlore	$Fd\bar{3}m$	10.59066(8)	2.67
64	Gd	Fluorite	$Fm\bar{3}m$	5.26142(6)	2.14

3.2. $Nd_2Zr_2O_7$

The order–disorder transition occurs at 2300 °C in the Nd_2O_3-ZrO_2 system [22,40], raising the possibility that it may be difficult to prepare $Nd_2Zr_2O_7$ single-crystals of the pyrochlore structure due to the relatively small difference between the melting point and the structural transition temperature (see Refs. [22,28]). When preparing this material it is therefore crucial to establish the crystallographic structure of the $Nd_2Zr_2O_7$ samples and to adjust the conditions of synthesis in order to prepare the desired phase, as has been emphasized in previous reports [40,41].

$Nd_2Zr_2O_7$ polycrystalline rods were sintered in air for 2 days at 1500 °C (below the structural transition temperature). Powder X-ray diffraction analysis showed that the feed rods have a cubic $Fd\bar{3}m$ pyrochlore structure and are single phase, with no additional peaks in the diffraction patterns.

The boules tended to have thermally generated cracks in most of the cases, regardless of the growth rate employed. The crystals developed facets as they grew and two very strong facets were present along almost the entire length of most of the crystals. The crystals were typically 5–7 mm in diameter and 55–65 mm long. A photograph of an as-grown crystal of $Nd_2Zr_2O_7$ prepared in air at a rate of 12.5 mm/h is shown in Fig. 3a.

Polarized light microscopy analysis of the cross section of the crystal with polished pieces cut from the boule of $Nd_2Zr_2O_7$ shows no evidence of the existence of grain boundaries, suggesting that the boule is monocrystalline. Macro-defects (cracks) observed on the crystal boules were probably caused by the large temperature gradient that exists inside the image furnace during the crystal growth.

The high quality of the $Nd_2Zr_2O_7$ crystals is also confirmed by X-ray Laue diffraction (see Fig. 3b). The Laue patterns indicate that in most cases the [1 1 1] direction is almost orthogonal to the facets seen on the sides of the as-grown crystal boules. Furthermore, we observed a natural preference of the crystal boules to cleave along the [1 1 1] crystallographic planes.

In order to ascertain whether the crystals formed in the pyrochlore or the defect-fluorite structure, powder X-ray diffraction measurements were carried out, and the pattern obtained for the ground crystal boule of $Nd_2Zr_2O_7$ is shown in Fig. 4. An analysis of the pattern made using the FullProf software suite provided a good fit (see Table 2) to the pyrochlore structure (space group $Fd\bar{3}m$). There were no impurity peaks observed in the pattern. The superlattice reflections (with ($h\,k\,l$)=(1 1 1), (3 3 1), and (5 1 1) characteristic to the pyrochlore structure were observed in the X-ray profile of $Nd_2Zr_2O_7$. Furthermore, the Bragg peaks are very sharp and no broadening of the reflections is observed [35]. We therefore conclude that there is no mixture of the two cubic crystallographic phases in any of the samples.

We also attempted to grow crystals of $Nd_2Zr_2O_7$ in oxygen, at a pressure of 2.5 bars. In this case, the growths were less stable and the resulting boules were of inferior quality.

Detailed crystallographic structural investigations of the $Nd_2Zr_2O_7$ single-crystals using neutron scattering and studies of the magnetic

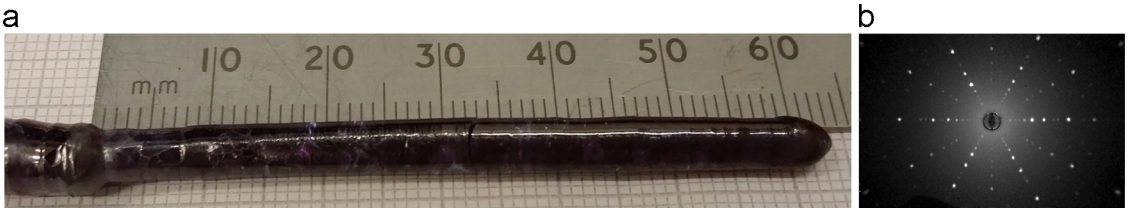

Fig. 3. (a) Crystal of $Nd_2Zr_2O_7$ grown in air at a rate of 12.5 mm/h. (b) X-ray Laue back reflection photograph of a crystal of $Nd_2Zr_2O_7$, showing the [1 1 1] orientation of an aligned sample used for magnetic properties measurements discussed in Ref. [42].

properties have been performed and the results are described elsewhere [42].

3.3. $Sm_2Zr_2O_7$

The Sm_2O_3–ZrO_2 system is similar to Nd_2O_3–ZrO_2, but in Sm compound, the order-disorder transition occurs at 2000 °C [22]. The small difference between the structural transition temperature and the melting point leads to difficulties in preparing single-crystals of the pyrochlore phase of $Sm_2Zr_2O_7$.

$Sm_2Zr_2O_7$ feed rods were sintered in air for 2 days at 1500 °C (below the order-disorder transition temperature). The results of the refinements obtained for the X-ray data on the $Sm_2Zr_2O_7$ polycrystalline powders show that no impurity phases are present in our polycrystalline precursors rods.

The as-grown samarium zirconate crystals were typically 5–7 mm in diameter and 30–90 mm long. As in the case of the neodymium zirconate growths, the $Sm_2Zr_2O_7$ boules tended to have cracks which are probably due to the large temperature gradient in the furnace during the crystal growth. The crystals developed facets as they grew and two very strong facets were present along almost the entire length of most of the crystals. A photograph of a crystal of $Sm_2Zr_2O_7$, which was grown in oxygen at a pressure of 4 bars and a growth speed of 8 mm/h, is shown in Fig. 5a. Fig. 5b shows a X-ray Laue photograph taken of a boule of $Sm_2Zr_2O_7$. The Laue patterns indicate that the [1 1 1] direction is nearly orthogonal to the facets seen on the sides of the as-grown crystal boule.

Fig. 6 shows the room temperature X-ray diffraction profile of a powdered crystal sample of $Sm_2Zr_2O_7$. The results of the refinement were similar to those obtained for the lanthanum and neodymium zirconates crystals. The weak superlattice reflections of the cubic $Fd\bar{3}m$ pyrochlore structure are clearly visible in the X-ray diffraction pattern and no impurity peaks were observed. The sharp Bragg peaks suggest that only the pyrochlore phase of $Sm_2Zr_2O_7$ crystal is formed.

Attempts to prepare single-crystals of $Sm_2Zr_2O_7$ in air proved to be unsuccessful. The growths were unstable and the resulting boules were of poor quality.

3.4. $Gd_2Zr_2O_7$

Due to the fact that in the Gd_2O_3–ZrO_2 system the order-disorder transition occurs at a lower temperature (1530 °C [22]) than the melting point, the synthesis of gadolinium zirconate with a pyrochlore structure has proven to be very difficult. Two polycrystalline rods were prepared and sintered at different temperatures.

The first set of $Gd_2Zr_2O_7$ feed rods were heated in air for 2 days at 1600 °C, which is above the structural transition temperature. Analysis of the X-ray diffraction patterns collected at room temperature on these rods showed that the cubic $Fm\bar{3}m$ defect-fluorite structure is formed.

In a second attempt, the polycrystalline rods were sintered in air for several days at 1450 °C (below the temperature of the structural transition), following the procedure described by Blanchard et al. [35]. In this case, the X-ray diffraction profiles reveal that the pyrochlore-type structure is formed.

We first tried to grow crystals of $Gd_2Zr_2O_7$ in air or oxygen atmospheres, using a double ellipsoidal IR furnace (NEC SC1MDH-11020, Canon Machinery Incorporated), equipped with two 3.5 kW halogen lamps. Temperatures of up to 2150 °C may be achieved at the sample position with this type of furnace [4]. These attempts failed due to the fact that the melting point of $Gd_2Zr_2O_7$ was not reached using this type of image furnace.

We have successfully grown crystals of $Gd_2Zr_2O_7$ using a four-mirror Xenon arc lamp optical image furnace. The gadolinium zirconate crystal boules grown were typically 5–6 mm in diameter

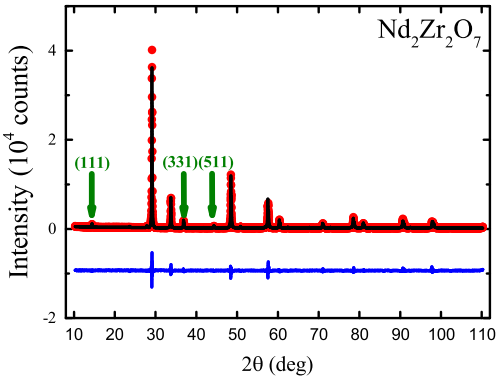

Fig. 4. Room temperature powder X-ray diffraction pattern collected on a ground boule of $Nd_2Zr_2O_7$. The experimental profile (red closed circles) and a full profile matching refinement (black solid line) are shown, with the difference given by the blue solid line. The pyrochlore superlattice reflections are indicated by the green arrows. (For interpretation of the references to color in this figure caption, the reader is referred to the web version of this paper.)

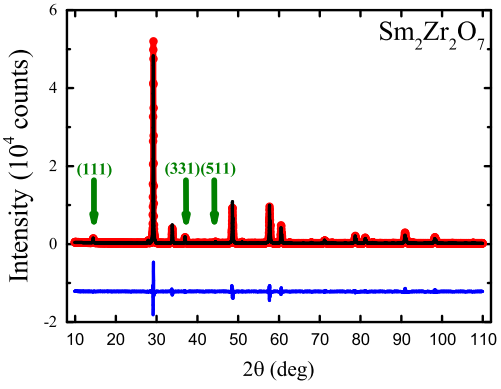

Fig. 6. Room temperature powder X-ray diffraction pattern collected for a $Sm_2Zr_2O_7$ crystal boule. The experimental profile (red closed circles) and a full profile matching refinement (black solid line) are shown, with the difference given by the blue solid line. The pyrochlore superlattice reflections are indicated by the green arrows. (For interpretation of the references to color in this figure caption, the reader is referred to the web version of this paper.)

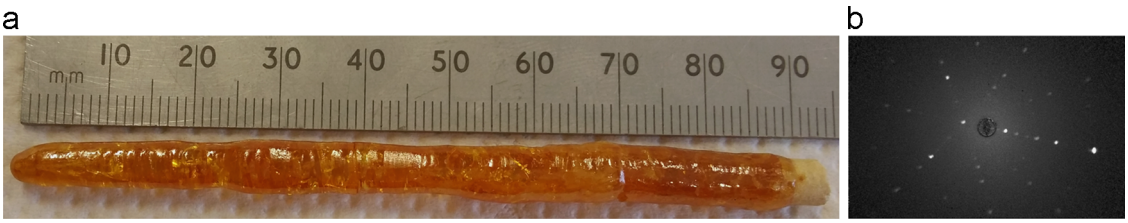

Fig. 5. (a) Boule of $Sm_2Zr_2O_7$ prepared in oxygen, at 4 bars pressure and using a growth rate of 8 mm/h. (b) X-ray Laue back reflection photograph taken for one of the facets of a $Sm_2Zr_2O_7$ crystal.

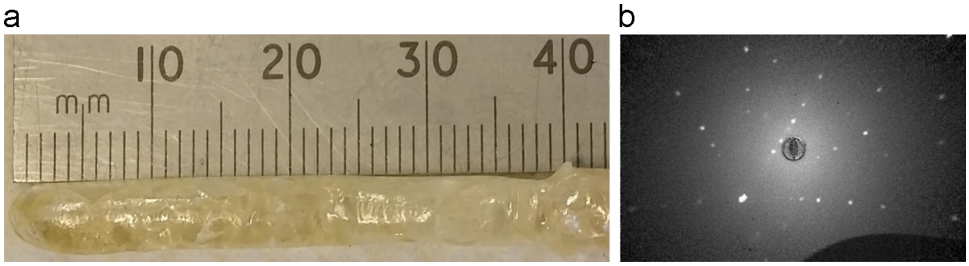

Fig. 7. (a) Crystal boule of $Gd_2Zr_2O_7$ prepared in air using a growth rate of 15 mm/h. (b) X-ray Laue back reflection photograph taken on a facet of a crystal of $Gd_2Zr_2O_7$.

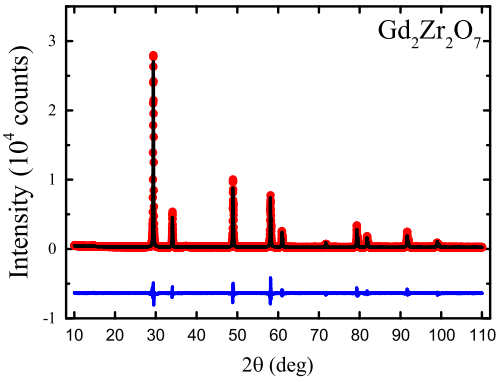

Fig. 8. Room temperature powder X-ray diffraction pattern collected on ground boules of $Gd_2Zr_2O_7$. The experimental profile (red closed circles) and a full profile matching refinement (black solid line), made using the $Fm\bar{3}m$ cubic structure are shown, with the difference given by the blue solid line. (For interpretation of the references to color in this figure caption, the reader is referred to the web version of this paper.)

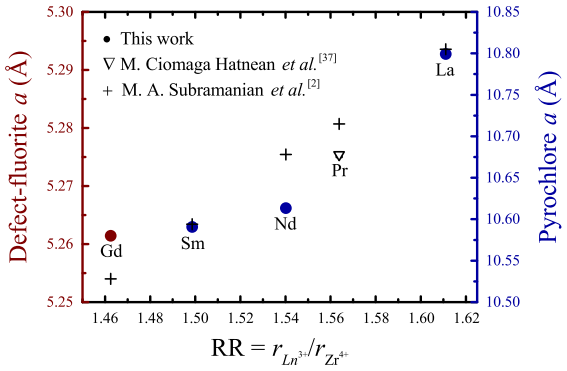

Fig. 9. Evolution of the lattice parameter, a, as a function of the ionic radius ratio, $RR = (r_{Ln^{3+}}/r_{Zr^{4+}})$. The ionic radius ratio, RR, were calculated using the values reported by Shannon et al. [43,44]. The previously reported values of the crystallographic parameters for the pyrochlore lanthanide zirconates series are given for comparison [2]. The lattice parameter of $Pr_2Zr_2O_7$ is also given for completeness [37].

and 30–40 mm long. Fig. 7a shows a photograph of a crystal of $Gd_2Zr_2O_7$, which was grown in air at a growth rate of 15 mm/h. Not all the crystals had facets. The X-ray Laue patterns (see Fig. 7b) indicate that the [1 1 1] direction is nearly orthogonal to the facets on the sides of this crystal boule.

In comparison to the other lanthanides in the pyrochlore zirconates series, no superlattice reflections characteristic of the pyrochlore structure were observed in the X-ray profile of $Gd_2Zr_2O_7$ (see Fig. 8), demonstrating that its lattice is best described by a defect-fluorite-type structure. In this case, the X-ray data were fitted to the cubic $Fm\bar{3}m$ space group.

Room temperature X-ray diffraction patterns collected on powdered pieces of the $Gd_2Zr_2O_7$ crystals prepared using both the feed rods sintered at 1600 °C and 1450 °C were identical. We therefore conclude that single-crystals of the gadolinium zirconate always form in the defect-fluorite structure, due to the fact that the order to disorder transition temperature is lower than the melting point of the $Gd_2Zr_2O_7$ phase.

3.5. Summary of X-ray diffraction results

The main results of the refinements of the room temperature X-ray data collected on the $Ln_2Zr_2O_7$ (where Ln=La, Nd, Sm, and Gd) crystals are listed in Table 2. The lattice parameter for the $Ln_2Zr_2O_7$ crystals of pyrochlore structure were found to be slightly smaller than the previously reported values for polycrystalline samples (see Fig. 9) [2,28], but this difference was also observed for $Pr_2Zr_2O_7$ samples prepared using different synthesis methods [37].

Fig. 9 shows the dependence of lattice parameter on the ionic radius ratio, $RR = (r_{Ln^{3+}}/r_{Zr^{4+}})$, for the crystals of lanthanide zirconates. The $Fd\bar{3}m$ cubic lattice parameter, a increases as the ionic radius ratio changes from 1.50 to 1.61 (Ln = Sm → La).

4. Conclusions

We have been successful in growing large, high quality crystals of lanthanide zirconates, $Ln_2Zr_2O_7$ (where Ln=La, Nd, Sm, and Gd) by the floating zone technique, using different growth conditions. The quality and composition of the as-grown boules was investigated using X-ray diffraction techniques. X-ray diffraction studies confirm that the crystallographic structure of the lanthanum, neodymium and samarium compounds (Ln= La, Nd, and Sm) corresponds to the pyrochlore structure, while the gadolinium zirconate $Gd_2Zr_2O_7$ crystal boule was obtained in the defect-fluorite form. The large size and the excellent quality of the grown crystals make them suitable for most physical properties characterization experiments. Detailed investigations of the low-temperature magnetic behavior of $Ln_2Zr_2O_7$ pyrochlores can be carried out on samples specifically aligned using the Laue technique.

Acknowledgments

This work was supported by a grant from the EPSRC, UK (EP/I007210/1). The authors thank T.E. Orton for valuable technical support.

References

[1] J.S. Gardner, M.J.P. Gingras, J.E. Greedan, Magnetic pyrochlore oxides, Rev. Mod. Phys. 82 (2010) 53.
[2] M.A. Subramanian, G. Aravamudan, G.V. Subba Rao, Oxide pyrochlores—a review, Prog. Solid State Chem. 15 (1983) 55.
[3] J.S. Gardner, B.D. Gaulin, D.M. Paul, Single crystal growth by the floating-zone method of a geometrically frustrated pyrochlore antiferromagnet, $Tb_2Ti_2O_7$, J. Cryst. Growth 191 (1998) 740.
[4] G. Balakrishnan, O.A. Petrenko, M.R. Lees, D.M. Paul, Single crystal growth of rare earth titanate pyrochlores, J. Phys.: Condens. Matter. 10 (1998) L723.
[5] D. Prabhakaran, A.T. Boothroyd, Crystal growth of spin-ice pyrochlores by the floating-zone method, J. Cryst. Growth 318 (2011) 1053.

[6] L.-J. Chang, S. Onoda, Y. Su, Y.-J. Kao, K.-D. Tsuei, Y. Yasui, K. Kakurai, M.R. Lees, Higgs transition from a magnetic Coulomb liquid to a ferromagnet in $Yb_2Ti_2O_7$, Nat. Commun. 3 (2012) 992.
[7] K.A. Ross, T. Proffen, H.A. Dabkowska, J.A. Quilliam, L.R. Yaraskavitch, J.B. Kycia, B.D. Gaulin, Lightly stuffed pyrochlore structure of single-crystalline $Yb_2Ti_2O_7$ grown by the optical floating zone technique, Phys. Rev. B 86 (2012) 174424.
[8] Q. Li, L. Xu, C. Fan, F. Zhang, Y. Lv, B. Ni, Z. Zhao, X. Sun, Single crystal growth of the pyrochlores $R_2Ti_2O_7$ (R=rare earth) by the optical floating-zone method, J. Cryst. Growth 377 (2013) 96.
[9] O.A. Petrenko, M.R. Lees, G. Balakrishnan, Magnetization process in the spin-ice compound $Ho_2Ti_2O_7$, Phys. Rev. B 68 (2003) 012406.
[10] H. Cao, A. Gukasov, I. Mirebeau, P. Bonville, C. Decorse, G. Dhalenne, Ising versus xy anisotropy in frustrated $R_2Ti_2O_7$ compounds as "seen" by polarized neutrons, Phys. Rev. Lett. 103 (2009) 056402.
[11] O.A. Petrenko, M.R. Lees, G. Balakrishnan, Titanium pyrochlore magnets: how much can be learned from magnetization measurements? J. Phys.: Condens. Matter 23 (2011) 164218.
[12] Y. Taguchi, K. Ohgushi, Y. Tokura, Optical probe of the metal–insulator transition in pyrochlore-type molybdate, Phys. Rev. B 65 (2002) 115102.
[13] I. Kézsmárki, N. Hanasaki, D. Hashimoto, S. Iguchi, Y. Taguchi, S. Miyasaka, Y. Tokura, Charge dynamics near the electron-correlation induced metal–insulator transition in pyrochlore-type molybdates, Phys. Rev. Lett. 93 (2004) 266401.
[14] Y. Taguchi, Y. Oohara, H. Yoshizawa, N. Nagaosa, Y. Tokura, Spin chirality, berry phase, and anomalous Hall effect in a frustrated ferromagnet, Science 291 (2001) 2573.
[15] K. Taniguchi, T. Katsufuji, S. Iguchi, Y. Taguchi, H. Takagi, Y. Tokura, Raman study of the metal–insulator transition in pyrochlore mo oxides, Phys. Rev. B 70 (2004) 100401 (R).
[16] N. Hanasaki, M. Kinuhara, I. Kézsmárki, S. Iguchi, S. Miyasaka, N. Takeshita, C. Terakura, H. Takagi, Y. Tokura, Mott–Anderson transition controlled by a magnetic field in pyrochlore molybdate, Phys. Rev. Lett. 96 (2006) 116403.
[17] S. Singh, R. Suryanarayanan, R. Tackett, G. Lawes, A.K. Sood, P. Berthet, A. Revcolevschi, Ordered spin-ice state in the geometrically frustrated metallic ferromagnet $Sm_2Mo_2O_7$, Phys. Rev. B 77 (2008) 020406 (R).
[18] R.C. Ewing, W.J. Weber, J. Lian, Nuclear waste disposal—pyrochlore ($A_2B_2O_7$): nuclear waste form for the immobilization of plutonium and "minor" actinides, J. Appl. Phys. 95 (2004) 5949.
[19] J. Wu, X. Wei, N.P. Padture, P.G. Klemens, M. Gell, E. Garcia, P. Miranzo, M.I. Osendi, Low-thermal-conductivity rare-earth zirconates for potential thermal-barrier-coating applications, J. Am. Ceram. Soc. 85 (2002) 3031.
[20] K. Kimura, S. Nakatsuji, J.-J. Wen, C. Broholm, M.B. Stone, E. Nishibori, H. Sawa, Quantum fluctuations in spin-ice-like $Pr_2Zr_2O_7$, Nat. Commun. 4 (2013) 1934.
[21] M.J.P. Gingras, P.A. McClarty, Quantum spin ice: a search for gapless quantum spin liquids in pyrochlore magnets, Rep. Prog. Phys. 77 (2014) 056501.
[22] D. Michel, M.P.Y. Jorba, R. Collongues, Etude de la transformation ordre-desordre de la structure fluorite a la structure pyrochlore pour des phases $(1-x)ZrO_2-xLn_2O_3$, Mater. Res. Bull. 9 (1974) 1457.
[23] D. Michel, M.P.Y. Jorba, R. Collongues, Study by raman spectroscopy of order–disorder phenomena occurring in some binary oxides with fluorite-related structures, J. Raman Spectrosc. 5 (1976) 163.
[24] M.J.D. Rushton, R.W. Grimes, Predicted pyrochlore to fluorite disorder temperature for $A_2Zr_2O_7$ compositions, J. Mater. Res. 19 (2004) 1603.
[25] N.R.S. Kumar, N.V.C. Shekar, P.C. Sahu, Pressure induced structural transformation of pyrochlore $Gd_2Zr_2O_7$, Solid State Commun. 147 (2008) 357.
[26] S. Surblé, S. Heathman, P.E. Raison, D. Bouëxière, K. Popa, R. Caciuffo, Pressure-induced structural transition in $Ln_2Zr_2O_7$(Ln = Ce, Nd, Gd) pyrochlores, Phys. Chem. Miner. 37 (2010) 761.
[27] H.Y. Xiao, F.X. Zhang, F. Gao, M. Lang, R.C. Ewing, W.J. Weber, Zirconate pyrochlores under high pressure, Phys. Chem. Chem. Phys. 12 (2010) 12472.
[28] R.S. Roth, Pyrochlore-type compounds containing double oxides of trivalent and tetravalent ions, J. Res. Natl. Bur. Stand. 56 (1956) 2643.
[29] H.W.J. Blöte, R.F. Wielinga, W.J. Huiskamp, Heat capacity measurements on rare-earth double oxides $R_2M_2O_7$, Physica 43 (1969) 549.
[30] K.K. Rao, T. Banu, M. Vithal, G.Y.S.K. Swamy, K.R. Kumar, Preparation and characterization of bulk and nano particles of $La_2Zr_2O_7$ and $Nd_2Zr_2O_7$ by sol–gel method, Mater. Lett. 54 (2002) 205.
[31] S. Lutique, P. Javorský, R.J.M. Konings, A.C.G. van Genderen, J.C. van Miltenburg, F. Wastin, Low temperature heat capacity of $Nd_2Zr_2O_7$ pyrochlore, J. Chem. Thermodyn. 35 (2003) 955.
[32] F.X. Zhang, J. Lian, U. Becker, L.M. Wang, J. Hu, S. Saxena, Structural distortions and phase transformations in $Sm_2Zr_2O_7$ pyrochlore at high pressures, Chem. Phys. Lett. 441 (2007) 216.
[33] A.M. Durand, P. Klavins, L.R. Corruccini, Heat capacity of the frustrated magnetic pyrochlores $Gd_2Zr_2O_7$ and $Gd_2Hf_2O_7$, J. Phys.: Condens. Matter 20 (2008) 235208.
[34] S. Singh, S. Saha, S.K. Dhar, R. Suryanarayanan, A.K. Sood, A. Revcolevschi, Manifestation of geometric frustration on magnetic and thermodynamic properties of the pyrochlores $Sm_2X_2O_7$ (X= Ti, Zr), Phys. Rev. B 77 (2008) 054408.
[35] P.E.R. Blanchard, R. Clements, B.J. Kennedy, C.D. Ling, E. Reynolds, M. Avdeev, A.P.J. Stampfl, Z. Zhang, L.-Y. Jang, Does local disorder occur in the pyrochlore zirconates? Inorg. Chem. 51 (2012) 13237.
[36] K. Matsuhira, C. Sekine, C. Paulsen, M. Wakeshima, Y. Hinatsu, T. Kitazawa, Y. Kiuchi, Z. Hiroi, S. Takagi, Spin freezing in the pyrochlore antiferromagnet $Pr_2Zr_2O_7$, J. Phys.: Conf. Ser. 145 (2009) 012031.
[37] M. Ciomaga Hatnean, C. Decorse, M.R. Lees, O.A. Petrenko, D.S. Keeble, G. Balakrishnan, Structural and magnetic properties of single crystals of the geometrically frustrated zirconium pyrochlore, $Pr_2Zr_2O_7$, Mater. Res. Express.
[38] S.M. Koohpayeh, J.-J. Wen, B.A. Trump, C.L. Broholm, T.M. McQueen, synthesis, floating zone crystal growth and characterization of the quantum spin ice $Pr_2Zr_2O_7$ pyrochlore, J. Cryst. Growth 402 (2014) 291.
[39] J. Rodríguez-Carvajal, Recent advances in magnetic structure determination by neutron powder diffraction, Physica B 192 (1993) 55–69.
[40] H. Ohtani, S. Matsumoto, B. Sundman, T. Sakuma, M. Hasebe, Equilibrium between fluorite and pyrochlore structures in the ZrO_2–Nd_2O_3 system, Mater. Trans. 46 (2005) 1167.
[41] J.L. Payne, M.G. Tucker, I.R. Evans, From fluorite to pyrochlore: characterisation of local and average structure of neodymium zirconate, $Nd_2Zr_2O_7$, J. Solid State Chem. 205 (2013) 29.
[42] M. Ciomaga Hatnean, M.R. Lees, O.A. Petrenko, D.S. Keeble, G. Balakrishnan, M. Gutmann, B.Z. Malkin, V.V. Klekovkina, Structural and magnetic investigations of single-crystals of the neodymium zirconate pyrochlore, $Nd_2Zr_2O_7$, 2015, submitted for publication.
[43] R.D. Shannon, C.T. Prewitt, Effective ionic radii in oxides and fluorides, Acta Crystallogr. B 25 (1969) 925.
[44] R.D. Shannon, Revised effective ionic radii and systematic studies of interatomic distances in halides and chaleogenides, Acta Crystallogr. A 32 (1976) 751.